

Nuclear effects in neutral current quasi-elastic neutrino interactions

Omar Benhar^{a,b}, Giovanni Veneziano^b

^a*INFN, Sezione di Roma, I-00185 Roma, Italy*

^b*Dipartimento di Fisica, “Sapienza” Università di Roma, I-00185 Roma, Italy*

Abstract

The interpretation of the charged (CCQE) and neutral (NCE) current quasi elastic events collected by the MiniBooNE collaboration involves a number of unresolved issues. While it has been suggested that the data can be explained in terms of an effective nucleon axial mass, M_A , the results of our theoretical calculations suggest that the CCQE and NCE samples cannot be described by the same value of M_A . We argue that the disagreement between theory and data may arise from the uncertainties associated with the flux average procedure. We also analyze the role of the strange quark in NCE interactions and find that, due to a cancellation between proton and neutron contributions, it turns out to be negligible.

Keywords:

neutrino-nucleus interactions, neutral current, nuclear effects
25.30.Pt, 13.15.+g, 24.10.Cn

1. Introduction

The MiniBooNE collaboration has recently collected an extensive data set of quasielastic neutrino nucleus scattering events, in both the charged-current (CCQE) [1] and neutral current (NCE) [2] channels, using a Carbon target.

In the CCQE channel, quasielastic neutrino-nucleon interactions are described in terms of the vector form factors $F_1^{p,n}(Q^2)$ and $F_2^{p,n}(Q^2)$ ($Q^2 = -q^2$, q being the four-momentum transfer, while the superscripts p and n correspond to proton and neutron, respectively), that have been precisely measured in electron-proton and electron-deuteron scattering experiments [3],

and the axial form factor $F_A(Q^2)$ [4, 5, 6]. In addition, NCE interactions are also affected by the form factors F_1^s , F_2^s and F_A^s , arising from strange quark contributions [7, 8, 9, 10]. The results of recent experiments [7] indicate that F_1^s , F_2^s are vanishing, whereas the axial form factors F_A and F_A^s are assumed to be of dipole form, and their Q^2 -dependence is parametrized in terms of the axial mass M_A .

The measured cross sections turn out to be consistently larger than the predictions of Monte Carlo simulations carried out using the relativistic Fermi gas (RFG) model of the nucleus and the value of the axial mass resulting from the world average of the deuterium data, $M_A = 1.03$ GeV [6]. In order to bring the predictions of the RFG model into agreement with the data, the authors of Refs.[1, 2] use a significantly larger value of the axial mass, $M_A \gtrsim 1.35$ GeV, and introduce the additional parameter κ , meant to improve the treatment of Pauli blocking. The K2K collaboration also reported a large value of the axial mass, $M_A \sim 1.2$ GeV, resulting from the analysis of its sample of CCQE events [11]. Moreover, the best fit to the neutral current data is obtained using a non vanishing strange quark contribution Δs , determining the value of F_A^s at $Q^2 = 0$ [2].

It has been suggested that the large value of M_A may be regarded as an *effective* axial mass, modified by nuclear effects not taken into account in the RFG model [1]. However, the results obtained using more advanced models appear to rule out this explanation. In fact, numerical calculations carried out using realistic nuclear spectral functions, extensively employed in the analysis of electron-nucleus scattering data [12], indicate that reproducing the CCQE measured cross sections requires an even larger value of M_A [13, 14].

The purpose of this work is the extension of the spectral function approach of Refs.[13, 14] to the description of NCE interactions and the quantitative analysis of the M_A and Δs dependence of the resulting cross sections. The main elements of our approach are outlined in Section 2, while the numerical results are discussed in Section 3. Finally, in Section 4 we summarize our findings and state the conclusions.

2. Formalism

We consider the neutral current process

$$\nu_\mu + {}^{12}\text{C} \rightarrow \nu_\mu + X, \quad (1)$$

in which a neutrino carrying initial four-momentum $k = (E_\nu, \mathbf{k})$ scatters off a Carbon target to a state of four-momentum $k' = (E'_\nu, \mathbf{k}')$, the target final state being undetected. In the impulse approximation (IA) scheme [15], stating that when the magnitude of the momentum transfer $|\mathbf{q}|$ is large enough (i) the target nucleus is seen by the probe as a collection of individual nucleons and (ii) in the final state the knocked out nucleon and the recoiling nucleus evolve independently of one another, the differential cross section can be written in the form

$$d\sigma_{IA} = \int d^3p dE P(\mathbf{p}, E) d\sigma_{elem} , \quad (2)$$

where $d\sigma_{elem}$ is the neutrino-nucleon cross section and $P(\mathbf{p}, E)$ is the spectral function of the target nucleus, yielding the probability distribution of finding a nucleon of momentum \mathbf{p} and removal energy E in the nuclear target.

2.1. Neutrino nucleon cross section

The NCE neutrino nucleon cross section in the center of mass frame reads

$$\frac{d\sigma_{elem}}{d\Omega} = \frac{|\bar{\mathcal{M}}|^2}{64\pi^2(E_\nu + E_p)^2} \left(\frac{E'}{E_\nu} \right) , \quad (3)$$

where E_p is the nucleon energy and $|\bar{\mathcal{M}}|$ is Feynman's invariant amplitude, averaged over the spins of the initial state particles and summed over the spins of the particles in the final state.

Feynman's amplitude can be written as

$$\mathcal{M} = \frac{i}{2\sqrt{2}} G_F \underbrace{\bar{\nu}(k') \gamma_\mu (1 - \gamma_5) \nu(k)}_{\text{leptonic current}} \underbrace{< N(p') | J_Z^\mu | N(p) >}_{\text{hadronic current}} , \quad (4)$$

where $\nu(k)$ and $\bar{\nu}(k')$ are the Dirac spinors associated with the initial and final state neutrino, respectively, the kets $|N(p) >$ and $|N(p') >$ represent the initial and final nucleon state, and J_Z is the hadronic neutral current. While the leptonic current has a simple V-A structure, completely determined by the leptons kinematics, the hadronic current is more complex, on account of the strong interactions occurring between the nucleon constituents.

The hadronic neutral weak current can be written in the general form

$$\begin{aligned} & < N(p') | J_Z^\mu | N(p) > = \\ & < N' | \left[\gamma^\mu F_1^z(Q^2) + \frac{i\sigma^{\mu\nu} q_\nu}{2M} F_2^z(Q^2) + \gamma^\mu \gamma^5 F_A^z(Q^2) \right] | N > , \end{aligned} \quad (5)$$

where $F_1^z(Q^2)$, $F_2^z(Q^2)$ and $F_A^z(Q^2)$ are the Dirac, Pauli and axial form factors for neutral current interactions, respectively, taking into account the strange quark content of the nucleon.

The form of the neutral weak current

$$J_Z = J_3 - 2\sin^2\theta_W J_{em} , \quad (6)$$

where J_3 , J_{em} and θ_W are the third component of the isospin current, the electromagnetic current and Weinberg's angle, respectively, suggests the following parametrization of the form factors

$$\begin{aligned} F_1^{z,p}(Q^2) &= \frac{1}{2} [\bar{F}_1(Q^2) - F_1^s(Q^2)] - 2\sin^2\theta_W F_1^p(Q^2), \\ F_1^{z,n}(Q^2) &= \frac{1}{2} [-\bar{F}_1(Q^2) - F_1^s(Q^2)] - 2\sin^2\theta_W F_1^n(Q^2), \\ F_2^{z,p}(Q^2) &= \frac{1}{2} [\bar{F}_2(Q^2) - F_2^s(Q^2)] - 2\sin^2\theta_W F_2^p(Q^2), \\ F_2^{z,n}(Q^2) &= \frac{1}{2} [-\bar{F}_2(Q^2) - F_2^s(Q^2)] - 2\sin^2\theta_W F_2^n(Q^2), \\ F_A^{z,p}(Q^2) &= \frac{1}{2} F_A(Q^2) - \frac{1}{2} F_A^s(Q^2), \\ F_A^{z,n}(Q^2) &= -\frac{1}{2} F_A(Q^2) - \frac{1}{2} F_A^s(Q^2), \end{aligned} \quad (7)$$

where

$$\bar{F}_i(Q^2) = F_i^p(Q^2) - F_i^n(Q^2) \quad i = 1, 2 , \quad (8)$$

and s indicates the strange quark contribution. As stated above, F_1^s and F_2^s are vanishing, while F_A^s is assumed to have a dipole Q^2 dependence

$$F_A^s(Q^2) = \frac{\Delta s}{\left(1 + \frac{Q^2}{M_A^2}\right)^2} , \quad (9)$$

Δs being the strange quark contribution to the nucleon spin at $Q^2 = 0$.

Following Ref. [8], we parametrize Feynman's amplitude \mathcal{M} in terms of six contributions according to

$$|\bar{\mathcal{M}}|^2 = 4G_F^2(V_{11} + V_{12} + V_{22} + A + V_{A1} + V_{A2}) , \quad (10)$$

with

$$\begin{aligned}
V_{11} &= 4(F_1^z)^2 [p \cdot k k' \cdot p' + p' \cdot k k' \cdot p - M^2 k \cdot k'] , \\
V_{12} &= -4F_1^z F_2^z k \cdot k' (p' - p) \cdot (k - k') , \\
V_{22} &= \frac{2(F_2^z)^2}{M^2} k \cdot k' [p \cdot k p' \cdot k + p \cdot k' p' \cdot k' + M^2 k \cdot k'] , \\
A &= 4(G_A)^2 [p \cdot k k' \cdot p' + p' \cdot k k' \cdot p + M^2 k \cdot k'] , \\
V_{A1} &= 8G_A F_1^z [p \cdot k p' \cdot k' - k \cdot p' p \cdot k'] , \\
V_{A2} &= 4G_A F_2^z k \cdot k' (k + k') \cdot (p + p') ,
\end{aligned} \tag{11}$$

where M is the nucleon mass and $G_A = -F_A^z(g_A - \Delta s)/(g_A + \Delta s)$, with $g_A = F_A(Q^2 = 0)$.

2.2. Target spectral function

Accurate *ab initio* calculations of the spectral function $P(\mathbf{p}, \mathbf{E})$, based on realistic nuclear hamiltonians, can only be carried out for the lightest nuclei ($A \leq 4$) [16, 17, 18, 19, 20, 21] and in the limit of uniform nuclear matter ($A \rightarrow \infty$) [22, 23]. In the case of medium-heavy nuclei, the calculation of $P(\mathbf{p}, \mathbf{E})$ involves severe difficulties, and one has to resort to some simplifying assumptions.

Within the RFG model [24, 25] the nucleus is described as a degenerate gas of non-interacting nucleons. According to this picture the spectral function takes the simple form

$$P_{RFGM}(\mathbf{p}, E) = \left(\frac{6\pi^2 A}{p_F^3} \right) \Theta(p_F - |\mathbf{p}|) \delta(E_{\mathbf{p}} - E_B + E) , \tag{12}$$

where $E_{\mathbf{p}} = \sqrt{M^2 + |\mathbf{p}|^2}$ is the energy of a free nucleon carrying momentum \mathbf{p} . The Fermi momentum p_F and the average binding energy E_B are the model parameters, to be adjusted to reproduce the experimental data.

The spectral function in Eq. 12 is non vanishing only at $|\mathbf{p}| < p_F$. However, electron-nucleus scattering experiments have provided unambiguous evidence of strong nucleon-nucleon correlations, that give rise to virtual scattering processes leading to the excitation of nucleons to states of large momentum and removal energy [12]. Hence, the quantitative analysis of neutrino-nucleus interactions requires a more realistic spectral function, taking into account correlation effects.

In our work we have used the Carbon spectral function of Ref.[26], obtained within the Local Density Approximation (LDA) combining the information extracted from measurements of the coincidence $(e, e'p)$ cross section with theoretical calculations of the spectral function of uniform nuclear matter at different densities.

The resulting $P(\mathbf{p}, E)$ consists of two contributions [26]

$$P_{LDA}(\mathbf{p}, E) = P_{MF}(\mathbf{p}, E) + P_{corr}(\mathbf{p}, E) , \quad (13)$$

arising from the nuclear mean field and from nucleon-nucleon correlation.

The mean field spectral function reads

$$P_{MF}(\mathbf{p}, E) = \sum_n Z_n |\phi_n(\mathbf{p})|^2 F_n(E - E_n) , \quad (14)$$

In the above equation, $\phi_n(\mathbf{p})$ is the squared momentum-space wave function of the n -th shell model state, whose width is described by the Lorentzian $F_n(E - E_n)$, Z_n is the corresponding spectroscopic factor and the sum extends to all states belonging to the Fermi sea. In the absence of correlation $Z_n \rightarrow 1$ and $F_n(E - E_n) \rightarrow \delta(E - E_n)$.

The correlation contribution to the LDA spectral function can be written in the form

$$P_{corr}(\mathbf{p}, E) = \int d^3r \rho_A(\mathbf{r}) P_{corr}^{NM}(\mathbf{p}, E; \rho = \rho_A(\mathbf{r})) , \quad (15)$$

where $\rho_A(\mathbf{r})$ is the nuclear density profile and $P_{corr}^{NM}(\mathbf{p}, E; \rho)$ is the correlation part of the nuclear matter spectral function at density ρ , whose calculation is described in Ref. [26]. Correlation effects turn out to be sizable, leading $\sim 20\%$ of the strength to the region of large momentum ($|\mathbf{p}| > p_F$) and large energy [26].

In the IA scheme statistical correlations leading to the suppression of the phase-space available to the final state nucleon, generally referred to as Pauli Blocking (PB), are not taken into account. In order to introduce their effect in our calculations, we have modified the spectral function according to [15]

$$P(\mathbf{p}, E) \Rightarrow P(\mathbf{p}, E) \Theta(|\mathbf{p} + \mathbf{q}| - \bar{p}_F) , \quad (16)$$

where \mathbf{q} is the momentum transfer and \bar{p}_F is the average Fermi momentum of the nucleus, defined as

$$\bar{p}_F = \int d^3r \rho_A(\mathbf{r}) p_F(\mathbf{r}) , \quad (17)$$

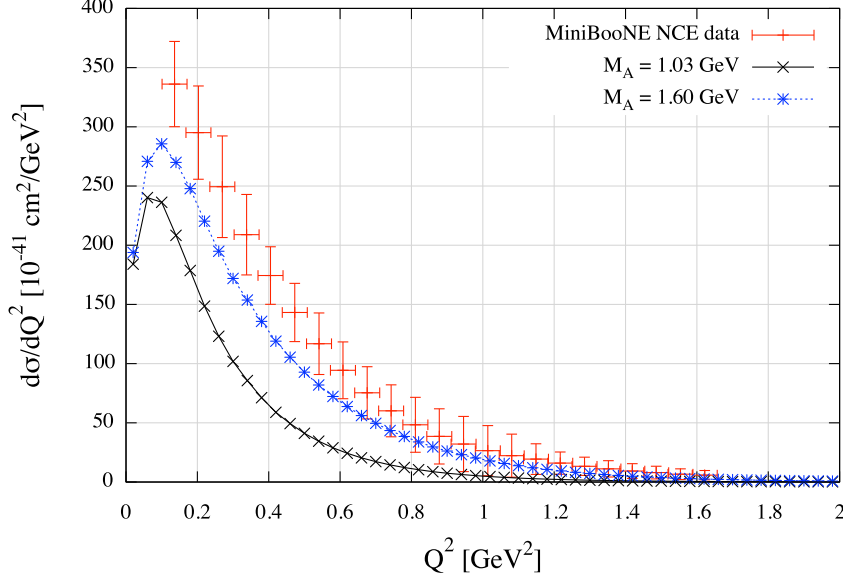


Figure 1: NCE flux averaged Q^2 -distribution for different values of the axial mass. The data points are taken from Ref. [2]

with

$$p_F(\mathbf{r}) = \left(\frac{3\pi^2 \rho_A(\mathbf{r})}{2} \right)^{1/3}. \quad (18)$$

For a Carbon target, Eqs. (17) and (18) lead to $\bar{p}_F = 225$ MeV. The inclusion of PB, while leaving unaffected the cross sections at large Q^2 , leads to an appreciable quenching in the region of low Q^2 [15].

3. Results

We have computed the Q^2 -distribution, averaged over the MiniBooNE flux, using the Carbon spectral function of Ref. [26]. Figure 1 shows the results corresponding to different values of the axial mass and $\Delta s = 0$, compared to the experimental data of Ref. [2]. It clearly appears that the value of the axial mass yielding a good fit of the MiniBooNE CCQE distribution, $M_A = 1.6$ GeV [14], does not reproduce NCE data.

To illustrate the dependence of our results on Δs , in Fig. 2 we show the flux averaged Q^2 -distribution for neutrinos interacting with a Carbon target,

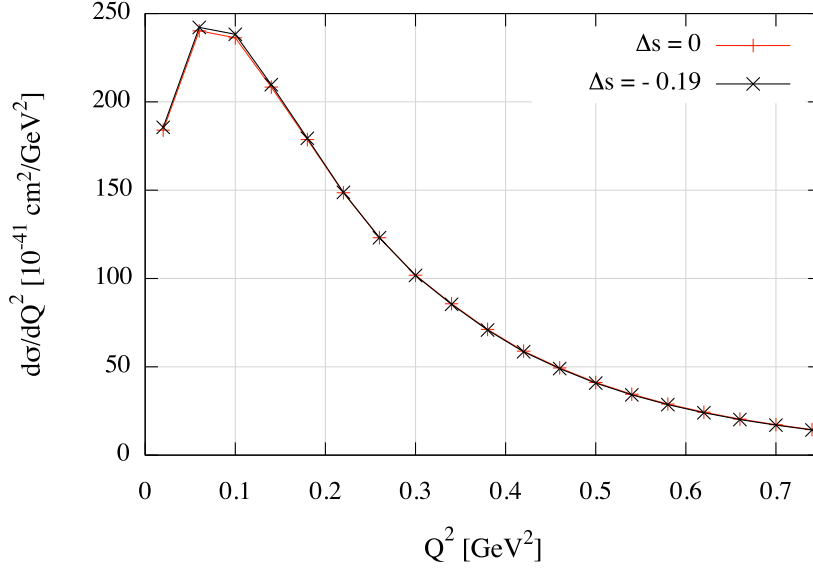


Figure 2: NCE flux averaged Q^2 -distribution for different values of Δs .

obtained using $M_A = 1.03$ GeV and setting $\Delta s = 0$ and $\Delta s = -0.19$, the latter being the lowest value that can be found in the literature [9, 10, 27].

It is apparent that the distribution is nearly independent of Δs . As a consequence, the results displayed in Fig. 1 have been obtained neglecting the strange quark contribution to the axial form factor.

In order to analyze the difference between the proton and neutron contributions, in Fig. 3 we show the same distributions as in Fig. 2, calculated for a $A = 12$ target consisting of protons or neutrons only. It turns out that the strange quark produces a suppression of the neutron contributions and an enhancement of the proton contribution of about the same size. As a result, the two effects largely cancel each other in the Carbon Q^2 -distribution, as seen in Fig. 2.

The role of strange quarks had been previously discussed in Refs. [8, 28], whose authors proposed to determine Δs from the ratio

$$\left(\frac{d\sigma}{dQ^2} \right)_{neutron}^{NCE} / \left(\frac{d\sigma}{dQ^2} \right)_{proton}^{NCE}, \quad (19)$$

that does not suffer from the uncertainties associated with the incoming

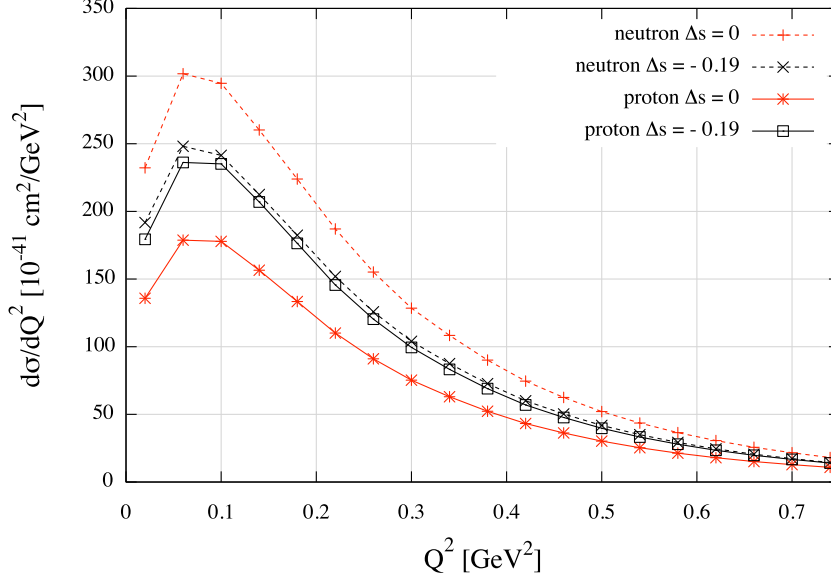


Figure 3: NCE proton and neutron contributions to the Carbon Q^2 -distribution.

neutrino flux and is very sensitive to variations of Δs .

4. Conclusions

Our work indicates that the theoretical analysis of the MiniBooNE NCE data sample involves the same difficulties already emerged in the studies of CCQE interactions [14].

The results discussed in Section 3, showing that it is impossible to describe both the CCQE and NCE data sets using the same value of the axial mass, confirm that nuclear effects not included in the oversimplified RFG model cannot be taken into account through a modification of M_A . In this context, it has to be pointed out that the need of a larger M_A to reproduce the measured NCE Q^2 -distribution is not likely to be ascribable to different nuclear effects in the CCQE and NCE channels. In fact, the ratio between the Q^2 -distributions obtained from the RFG model and the spectral function approach, providing a measure of the effects of nuclear dynamics, turns out to be nearly identical for CCQE and NCE. The difference does not exceed 2% over the whole Q^2 range.

Our analysis also shows that the strange quark contribution to the cross section of nuclei with equal number of protons and neutrons is vanishingly small. As a consequence, the possibility of improving the agreement between MC simulations and Carbon data adjusting the value of Δs appears to be ruled out.

The authors of Ref.[14] argued that the disagreement between theory and MiniBooNE CCQE data may be due to the uncertainties associated with the flux average procedure, as the resulting cross section at fixed energy and scattering angle of the outgoing muon picks up contributions from different kinematical regions, where different reaction mechanisms are known to be dominant.

This uncertainty also affects the flux averaged NCE differential cross section, which is given in bins of *reconstructed* Q^2 [2], defined as

$$Q_{rec}^2 = 2MT = 2M \sum_i T_i , \quad (20)$$

where M is the nucleon mass and T is the sum of the kinetic energies of the final state nucleons.

In order to provide results that can be compared to data in a meaningful fashion, theoretical models of neutrino-nucleus interactions must be based on a consistent description of the broad kinematical range corresponding to the relevant neutrino energies. In the quasi elastic sector, this amounts to taking into account, besides single-nucleon knock out, multi-nucleon knock out as well as processes involving the nuclear two-body currents, whose contribution is expected to be significant [29].

References

- [1] A.A. Aguilar-Arevalo *et al.* (MiniBooNE Collaboration), Phys. Rev. D **81** (2010) 092005.
- [2] A.A. Aguilar-Arevalo *et al.* (MiniBooNE Collaboration), Phys. Rev. D **82** (2010) 092005.
- [3] C.F. Perdrisat, V. Punjabi and M. Vanderhaeghen, Prog. Part. Nucl. Phys. **59** (2007) 694.
- [4] V. Bernard *et al.*, J. Phys. G **28** (2002) R1.

- [5] A. Bodek, S. Avvakumov, R. Bradford, and H. Budd, Eur. Phys. J. C **53** (2008) 349.
- [6] V. Lyubushkin et al. (NOMAD Collaboration), Eur. Phys. J. C **63** (2009) 355.
- [7] A. Acha *et al*, Phys. Rev. Lett. **98** (2007) 032301.
- [8] C.J. Horowitz, H. Kim, D.P. Murdock and S. Pollock, Phys. Rev. C **48** (1993) 3078.
- [9] W.M. Alberico *et al*, Nucl. Phys. **A651** (1999) 277.
- [10] K.F. Liu, J. Phys. G **27** (2001) 511.
- [11] R. Gran *et al*. (K2K Collaboration), Phys. Rev. D **74** (2006) 052002.
- [12] O. Benhar, D. Day and I. Sick, Rev. Mod. Phys. **80** (2008) 189.
- [13] O. Benhar and D. Meloni, Phys. Rev. D **80** (2009) 073003.
- [14] O. Benhar, P. Coletti and D. Meloni, Phys. Rev. Lett. **105** (2010) 132301.
- [15] O. Benhar, N. Farina, H. Nakamura, M. Sakuda and R. Seki, Phys. Rev. D **72** (2005) 053005.
- [16] A. E. L. Dieperink, T. de Forest and I. Sick, Phys. Lett. **B63** (1976) 261.
- [17] C. Ciofi degli Atti, E. Pace and G. Salm, Phys. Rev. C **21** (1980) 805.
- [18] H. Meier-Hajduk, Ch. Hajduk and P. U. Sauer, Nucl. Phys. **A395** (1983) 332.
- [19] C. Ciofi degli Atti, S. Liuti and S. Simula, Phys. Rev. C **41** (1990) R2474.
- [20] H. Morita and T. Suzuki, Prog. Theor. Phys. **86** (1991) 671.
- [21] O. Benhar and V. R. Pandharipande, Phys. Rev. C **47** (1993) 2218.
- [22] O. Benhar, A. Fabrocini and S. Fantoni, Nucl. Phys. **A505** (1989) 267.

- [23] A. Ramos, A. Polls and W.H. Dickhoff, Nucl. Phys **A503** (1989) 1.
- [24] R. A. Smith and E. J. Moniz, Nucl. Phys. **B43** (1972) 605 [Erratum-ibid. **B101** (1975) 547].
- [25] E. J. Moniz, Phys. Rev. **184** (1969) 1154.
- [26] O. Benhar, A. Fabrocini, S. Fantoni and I. Sick, Nucl. Phys. **A579** (1994) 493.
- [27] L. A. Ahrens, *et al.*, Phys. Rev. D **35** (1987) 785.
- [28] G.T. Garvey *et al.*, Phys. Lett. B **289** (1992) 249.
- [29] J.E. Amaro, M.B. Barbaro, J.A. Caballero, T.W. Donnelly and C.F. Williamson, Phys. Lett. **B696** (2011) 151.